

Deeply virtual scattering in QCD

VÍCTOR MARTÍNEZ-FERNÁNDEZ

PHD STUDENT AT THE NATIONAL CENTRE FOR NUCLEAR RESEARCH
(NCBJ, WARSAW, POLAND)



Outline

- Standard model: EW + QCD
- QCD \rightarrow deep inelastic scattering (**DIS**)
- Deeply virtual Compton scattering (**DVCS**) and collinear factorization:
 - The $x = \xi$ restriction
- Timelike Compton scattering (**TCS**)
- Double deeply virtual Compton scattering (**DDVCS**):
 - $x \neq \xi$ solution
 - Kleiss & Stirling (KS) techniques
 - **Latest results on theory and phenomenology**
- Experiments around the globe
- Summary

Standard model

Modern particle physics = Standard model:

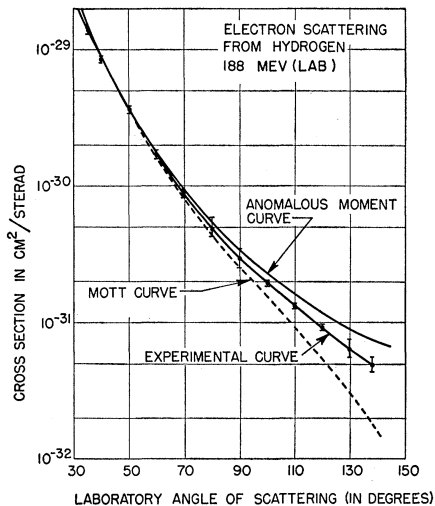
$$\underbrace{SU(3)_c}_{\text{QCD sector}} \otimes \underbrace{SU(2)_L \otimes U(1)_Y}_{\text{Electroweak sector}}$$

- $SU(3)_c$: strong interactions = quarks and gluons (*partons*) coupled to form hadrons
- Quarks and gluons: elementary, free *asymptotically* only
- Hadrons: composite objects, the states you find in nature

How to access partons?

- “Hitting” hadrons with high-energy particles: (virtual) photon
- Mid 1950s: SLAC proves the proton to be an extended object (**elastic scattering**)
- Late 1960s: SLAC & MIT prove the composite nature of the proton via **inelastic** scattering:
 - 1 Inclusive: **no control over all** final state particles
 - 2 Exclusive: **full control** over all final state particles

Elastic scattering of electron and proton at SLAC



Plot from: R. Hofstadter & R. W. McAllister, Phys. Rev. **98**, 217 (1955)

- Mott xsec: spinless and pointlike target

$$\left. \frac{d\sigma}{d\Omega} \right|_{\text{Mott}} = \underbrace{\frac{Z^2 \alpha_{\text{em}}^2}{4E^2 \sin^2(\theta/2)}}_{\text{Rutherford}} \cos^2(\theta/2)$$

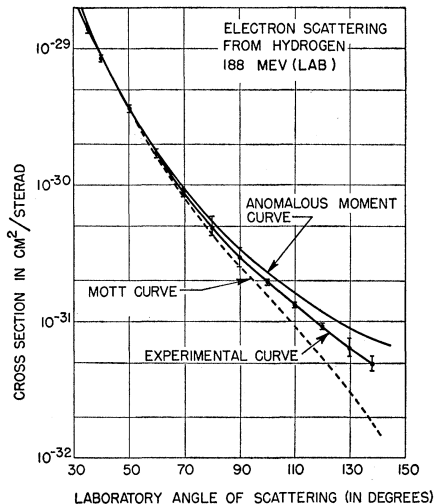
- Rosenbluth xsec: spin-1/2 and pointlike target

$$\left. \frac{d^2\sigma}{d\Omega dE'} \right|_{\text{Ros, point}} = \left. \frac{d\sigma}{d\Omega} \right|_{\text{Mott}} \left[1 + 2 \frac{Q^2}{4M^2} \tan^2(\theta/2) \right] \times \delta \left(\frac{Q^2}{2M} - \nu \right), \quad \nu = E - E'$$

- Rosenbluth xsec: spin-1/2 and extended target

$$\left. \frac{d^2\sigma}{d\Omega dE'} \right|_{\text{Ros, extended}} = \left. \frac{d\sigma}{d\Omega} \right|_{\text{Mott}} \left[F_E^2(|\vec{q}|^2) + 2 \frac{Q^2}{4M^2} \tan^2(\theta/2) F_M^2(|\vec{q}|^2) \right] \delta \left(\frac{Q^2}{2M} - \nu \right)$$

Elastic scattering of electron and proton at SLAC



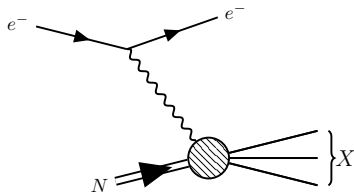
Plot from: R. Hofstadter & R. W. McAllister, Phys. Rev. **98**, 217 (1955)

- Rosenbluth xsec: spin-1/2 and extended target

$$\left. \frac{d^2\sigma}{d\Omega dE'} \right|_{\text{Ros, extended}} = \left. \frac{d\sigma}{d\Omega} \right|_{\text{Mott}} \left[F_E^2(|\vec{q}|^2) + 2 \frac{Q^2}{4M^2} \tan^2(\theta/2) F_M^2(|\vec{q}|^2) \right] \delta\left(\frac{Q^2}{2M} - \nu\right)$$

- Taking the **proton to be an extended object** of radius $\sim 10^{-13}$ cm with spin-1/2 fits the experimental data

Deep inelastic scattering (DIS)



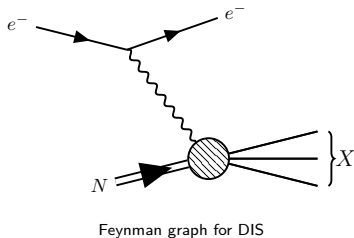
Feynman graph for DIS

- DIS: inclusive experiment breaking the proton

$$d\sigma_{\text{DIS}} \sim L^{\mu\nu} W_{\mu\nu}$$

- $L^{\mu\nu} \rightarrow$ pQED tensor, calculable
- $W_{\mu\nu} \rightarrow$ non-trivial QCD part: perturbative coefficient function convoluted with a non-perturbative term (PDF)

Deep inelastic scattering (DIS)



- DIS: inclusive experiment breaking the proton

$$d\sigma_{\text{DIS}} \sim L^{\mu\nu} W_{\mu\nu}$$

- $W_{\mu\nu} \rightarrow$ optical theorem:

$$\sum_X \int_X \left| \begin{array}{c} \text{wavy line} \\ \text{shaded vertex} \\ N \end{array} \right|^2 = 2\text{Im} \left(\begin{array}{c} \text{wavy line} \\ \text{shaded vertex} \\ N \end{array} \right)$$

$$\sum_X \int_X |X\rangle \langle X| = 1 \leftrightarrow \text{inclusiveness in practice}$$

Form factors & geometric shape

- DIS cross-section in terms of form factors (F_1, F_2):

$$\left. \frac{d^2\sigma}{d\Omega dE'} \right|_{\text{DIS}} = \left. \frac{d\sigma}{d\Omega} \right|_{\text{Mott}} \cdot \left[\frac{1}{\nu} F_2(x, Q^2) + \frac{2}{M} \tan^2(\theta/2) F_1(x, Q^2) \right],$$

$$x = \frac{Q^2}{2pq} \underbrace{=}_{\substack{\text{proton} \\ \text{rest} \\ \text{frame}}} \frac{Q^2}{2M\nu} \leftrightarrow \text{Björken variable},$$

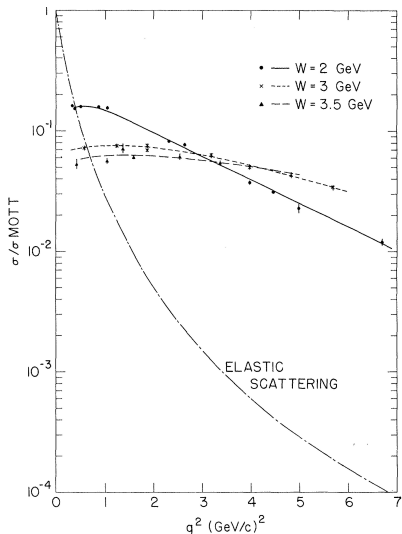
$$\nu = E - E'$$

- If F_1, F_2 are independent of Q^2 , then DIS results on scattering on pointlike particles and the proton is not elementary:

$$\text{spatial distribution: } \rho_j(\vec{r}) \sim \int d^3\vec{q} e^{i\vec{q}\vec{r}} F_j(x, |\vec{q}|^2), \quad |\vec{q}|^2 = Q^2$$

- If $F_j(x, |\vec{q}|^2) = f_j(x)$, then $\rho_j(\vec{r}) \sim \delta(\vec{r}) f_j(x) \Rightarrow$ pointlike target

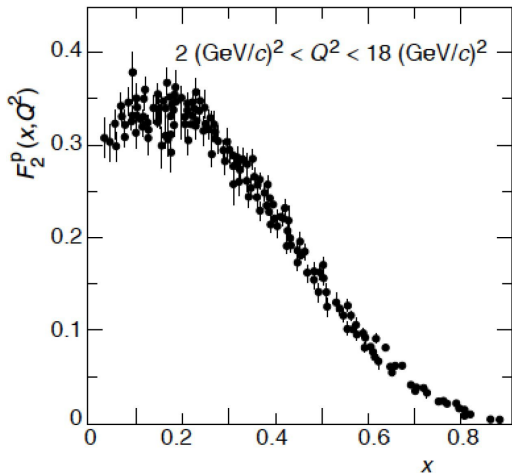
DIS at SLAC-MIT



Plot from: M. Breidenbach et al.,
Phys. Rev. Lett. **23**, 935 (1969)

- W is the invariant mass of the recoiling target system (X in the graph for DIS)
- **$W = 3$ and 3.5 GeV:** the (almost) independence with q^2 suggests scattering off elementary particles (pointlike or very small) particles

More from SLAC



Plot taken from Carolina Riedl's talk at the 61 Cracow summer school of theoretical physics: Electron-Ion Collider physics (2021). F_2^p means F_2 for the proton

- Almost independent of Q^2 : very small particles inside the proton that are interacting with each other, i.e.,

$$F_2(x, Q^2) \sim F_2(x)$$

- Dependence on $Q^2 \rightarrow$ DGLAP and gluons

Parton Distribution Function (PDF)

- DIS cross-section can be factorized via PDFs as

$$\sigma_{\gamma N \rightarrow X} = \sum_f \int_0^1 dx \sigma_{\gamma q_f \rightarrow X}(x) \text{PDF}_f(x), \quad f = \text{flavor},$$

$x = \text{longitudinal momentum fraction},$

in the Björken limit: $Q^2 \rightarrow \infty, x \text{ fixed}$

- For PDFs, x coincides with the Björken variable: $x_B = \frac{Q^2}{2pq}$
- PDF is a 1D distribution:

$$\text{PDF}_f(x) = \frac{1}{2} \int \frac{dz^-}{2\pi} e^{ix\bar{p}^+ z^-} \langle N(p) | \bar{q}_f(-z/2) \gamma^+ \mathcal{W}[-z/2, z/2] q_f(z/2) | N(p) \rangle \Big|_{z_\perp = z^+ = 0}$$

- z^+, z^-, z_\perp : light-cone coordinates
- \mathcal{W} : Wilson line

Light-cone dominance

- In PDF: $z^2 = 2z^+z^- + z_\perp^2 \xrightarrow{z^+=z_\perp=0} 0$, **but why?**
- PDF comes from $W_{\mu\nu}$:

$$4\pi W_{\mu\nu} = \int d^4z e^{iqz} \langle p | j_\mu(z) j_\nu(0) | p \rangle$$

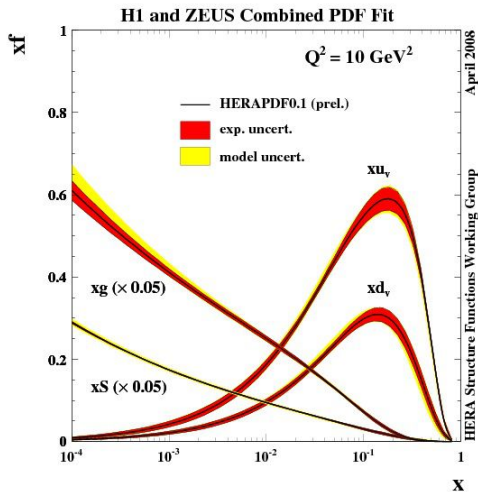
Light-cone dominance

$$4\pi W_{\mu\nu} = \int d^4z e^{iqz} \langle p | j_\mu(z) j_\nu(0) | p \rangle$$

What's the support of this integral?

- 1 Causality: $z^2 \geq 0$
- 2 $qz = \frac{z^+\nu}{p^+} - z^- x_B p^+$, $\nu = pq \rightarrow \infty$ in Bj. lim.
- 3 Riemann-Lebesgue: $\int d^n z f(z) e^{-i\eta z} \xrightarrow{|\eta| \rightarrow \infty} 0$
- 4 qz must be small $\Rightarrow z^+ \sim p^+/\nu \sim 0$, $z^- \sim \text{const}/(x_B p^+)$
- 5 $qz \sim \text{const} < \infty$
- 6 $z^2 \sim z_\perp^2 = -((z^1)^2 + (z^2)^2) \leq 0$
- 7 (1) + (6) $\rightarrow z^2 \sim 0 \Rightarrow$ **DIS is light-cone dominated**

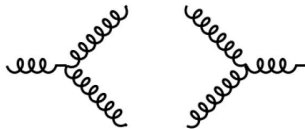
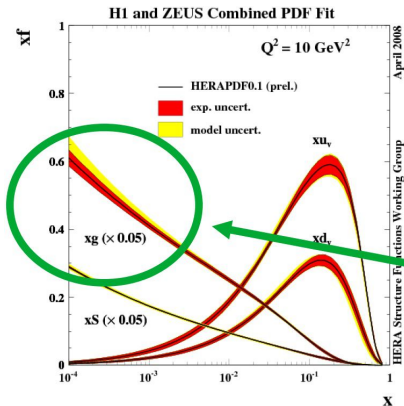
HERA's PDFs



- HERA = Hadron-Electron Ring Accelerator, at DESY in Germany
- Measurements of PDFs are key for experiments and calculations where hadrons play a role: pp collisions at the LHC are a primary example

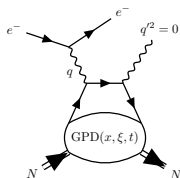
HERA's PDFs

- At small- x , there must be a saturation scale Q_s^2 for which gluon splitting and fusion rates become equal and the gluon distribution for momentum xg stops growing:



Deeply virtual Compton scattering (DVCS)

- In the late 1990s, Ji, Müller and Radyushkin introduced the Generalized Parton Distributions (GPDs) through the DVCS process:



Feynman diagram for DVCS

- It is an exclusive scattering
- $\xi = \frac{-\bar{q}\Delta}{2\bar{p}\bar{q}}$, $\bar{q} = \frac{q+q'}{2}$, $\bar{p} = \frac{p+p'}{2}$, $\Delta = p' - p$, $t = \Delta^2$

Relevance of the GPDs

- Connected to QCD energy-momentum tensor, and so to spin. GPDs are a way to address the hadron's **spin puzzle**. Ji's sum rule:

$$\int_{-1}^1 dx \ x [H_f(x, \xi, 0) + E_f(x, \xi, 0)] = 2J_f$$

- **Tomography**: distribution of quarks in terms of the longitudinal momentum and in the transverse plane,

$$q_f(x, \mathbf{b}_\perp) = \int \frac{d^2 \Delta}{4\pi^2} e^{-i\mathbf{b}_\perp \cdot \Delta} H_f(x, 0, t = -\Delta^2)$$

But how do GPDs appear?

DVCS amplitude

- To 1st order in α_{em} and under collinear factorization

($\mathcal{O}\left(\frac{\ell_{\perp}^2}{Q^2}, \frac{\Delta_{\perp}^2}{Q^2}, \frac{\ell_{\perp}\Delta_{\perp}}{Q^2}, \frac{\ell^-\bar{p}^+}{Q^2}\right)$ neglected):

$$\langle \gamma(q') N(p') | \mathcal{S}^{(2)} | \gamma^*(q) N(p) \rangle = -3i(2\pi)^4 \delta(p+q-p'-q') \sum_f e_f^2 (\varepsilon_{q\lambda})_{\alpha} (\varepsilon_{q'\lambda'}^*)_{\beta}$$

$$\times g_{\perp}^{\alpha\beta} \int_{-1}^1 dx \left(\frac{1}{x-\xi+i0} + \frac{1}{x+\xi-i0} \right) \underbrace{\frac{1}{2} \int \frac{dz^-}{2\pi} e^{ix\bar{p}^+z^-} \langle N(p') | \bar{q}_f(-z/2) \gamma^+ q_f(z/2) | N(p) \rangle}_{\text{GPD}} \Bigg|_{\substack{z^+=0 \\ z_{\perp}=0}}$$

+ (axial term)

- GPD factorization happens in the amplitude as opposed to the factorization in cross-section via PDFs
- GPD \simeq 3D version of a PDF

GPD & Compton Form Factor (CFF)

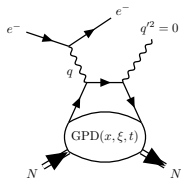
- CFF definition from our previous result ($t = \Delta^2$),

$$\text{CFF}(\xi, t) = \mathcal{H}_f(\xi, t) = \int_{-1}^1 dx \underbrace{\left(\frac{1}{x - \xi + i0} + \frac{1}{x + \xi - i0} \right)}_{\text{Coefficient function, } C_f(x, \xi), \text{ perturbative component}} \times \underbrace{H_f(x, \xi, t)}_{\text{a particular GPD}(x, \xi, t), \text{ non-perturbative function}}$$

- In observables, GPDs will appear hidden inside CFFs

The need to go beyond DVCS

- LO amplitude for DVCS restricts the access to GPDs to the line $x = \xi$:

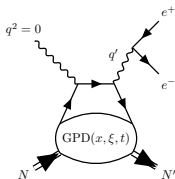


$$\text{CFF}_{\text{DVCS}} \sim \text{PV} \left(\int_{-1}^1 dx \frac{1}{x-\xi} \text{GPD}(x, \xi, t) \right) - \int_{-1}^1 dx i\pi \delta(x-\xi) \text{GPD}(x, \xi, t) + \dots$$

- Let us take a look at other processes that may solve this problem

Timelike Compton scattering (TCS)

- “Mirror” image of DVCS:



Feynman diagram for TCS

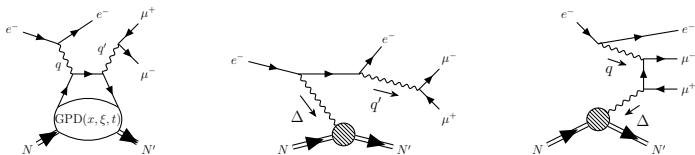
- GPDs enter the LO amplitude of TCS via the CFFs:

$$\text{CFF}_{\text{TCS}} \sim \text{PV} \left(\int_{-1}^1 dx \frac{1}{x+\xi} \text{GPD}(x, \xi, t) \right) - \int_{-1}^1 dx i\pi \delta(x+\xi) \text{GPD}(x, \xi, t) + \dots$$

- **1st measurement of TCS** by the CLAS collaboration at JLab: P. Chatagnon et al., PRL **127**, 262501 (2021)

Double deeply virtual Compton scattering (DDVCS)

- An extra virtuality with respect to DVCS and TCS to escape the $x = \pm\xi$ lines:



DDVCS (left), BH diagrams (middle and right). Crossed diagrams are not shown

- GPDs enter the DDVCS amplitude at LO via CFFs:

$$\text{CFF}_{\text{DDVCS}} \sim \text{PV} \left(\int_{-1}^1 dx \frac{1}{x-\rho} \text{GPD}(x, \xi, t) \right) - \int_{-1}^1 dx i\pi \delta(x-\rho) \text{GPD}(x, \xi, t) + \dots$$

$$\rho = -\frac{\bar{q}^2}{2\bar{p}\bar{q}}, \quad \xi = \frac{-\bar{q}\Delta}{2\bar{p}\bar{q}}$$

Original papers in DDVCS: Belitsky & Muller, PRL 90, 022001 (2003); Guidal & Vanderhaeghen, PRL 90, 012001 (2003); Belitsky & Muller, PRD 68, 116005 (2003)

DDVCS subprocess

- DDVCS subprocess amplitude:

$$i\mathcal{M}_{\text{DDVCS}} = \frac{ie^4 \bar{u}(\ell_-, s_\ell) \gamma_{\mu\nu} u(\ell_+, s_\ell) \bar{u}(k', s) \gamma_{\nu\mu} u(k, s)}{(q^2 + i0)(q'^2 + i0)} T_{s_2 s_1}^{\mu\nu}$$

- Compton tensor decomposition at LT:

$$T_{s_2 s_1}^{\mu\nu} = T^{(V)\mu\nu} \bar{u}(p', s_2) \left[(\mathcal{H} + \mathcal{E}) \not{h} - \frac{\mathcal{E}}{M} \bar{p}^+ \right] u(p, s_1) + T^{(A)\mu\nu} \bar{u}(p', s_2) \left[\tilde{\mathcal{H}} \not{h} + \frac{\tilde{\mathcal{E}}}{2M} \Delta^+ \right] \gamma^5 u(p, s_1)$$

$$T^{(V)\mu\nu} = -\frac{1}{2} (g^{\mu\nu} - n^\mu n^{*\nu} - n^\nu n^{*\mu}) \equiv -\frac{1}{2} g_\perp^{\mu\nu}$$

$$T^{(A)\mu\nu} = -\frac{i}{2} \epsilon^{\mu\nu\rho\sigma} n^\rho n^{*\sigma} \equiv -\frac{i}{2} \epsilon_\perp^{\mu\nu}$$

- Longitudinal plane is built with $\{\bar{q}, \bar{p}\}$
- $q_\perp^\nu \sim \Delta_\perp^\nu \Rightarrow g_\perp^{\mu\nu} q_\nu \neq 0 \Rightarrow$ EM gauge-violation

- Longitudinal plane is built with $\{\bar{q}, \bar{p}\}$
- $q_{\perp}^{\nu} \sim \Delta_{\perp}^{\nu} \Rightarrow g_{\perp}^{\mu\nu} q_{\nu} \neq 0 \Rightarrow$ EM gauge-violation
- Gauge-violation can be cured by evaluating the **hard part of the process** at $t = t_0$ ($|t_0| \leq |t|$):

$$q_{\perp}^{\nu}|_{t=t_0} \sim \Delta_{\perp}^{\nu}|_{t=t_0} = 0$$

- This procedure is consistent with the collinear factorization which is at the core of the GPD description

Kleiss-Stirling (KS) techniques

- Avoid computation of traces of gamma-matrices
- Address amplitude first instead of its modulus squared
- **Reduce amplitudes to complex-numbers**
- 2 scalars as building blocks, a and b as light-like vectors:

$$s(a, b) = \bar{u}(a, +)u(b, -) = -s(b, a)$$

$$t(a, b) = \bar{u}(a, -)u(b, +) = [s(b, a)]^*$$

$$s(a, b) = (a^2 + ia^3) \sqrt{\frac{b^0 - b^1}{a^0 - a^1}} - (a \leftrightarrow b)$$

Kleiss & Stirling, Nucl. Phys. B 262 (1985) 235-262

DDVCS subprocess à la KS

- DDVCS subprocess amplitude:

$$i\mathcal{M}_{\text{DDVCS}} = \frac{-ie^4}{(Q^2 - i0)(Q'^2 + i0)} \left(i\mathcal{M}_{\text{DDVCS}}^{(V)} + i\mathcal{M}_{\text{DDVCS}}^{(A)} \right)$$

- Vector contribution:

$$i\mathcal{M}_{\text{DDVCS}}^{(V)} = -\frac{1}{2} \left[f(s_\ell, \ell_-, \ell_+; s, k', k) - g(s_\ell, \ell_-, n^*, \ell_+) g(s, k', n, k) - g(s_\ell, \ell_-, n, \ell_+) g(s, k', n^*, k) \right] \\ \times \left[(\mathcal{H} + \mathcal{E}) [Y_{s_2 s_1} g(+, r'_{s_2}, n, r_{s_1}) + Z_{s_2 s_1} g(-, r'_{-s_2}, n, r_{-s_1})] - \frac{\mathcal{E}}{M} \mathcal{J}_{s_2 s_1}^{(2)} \right]$$

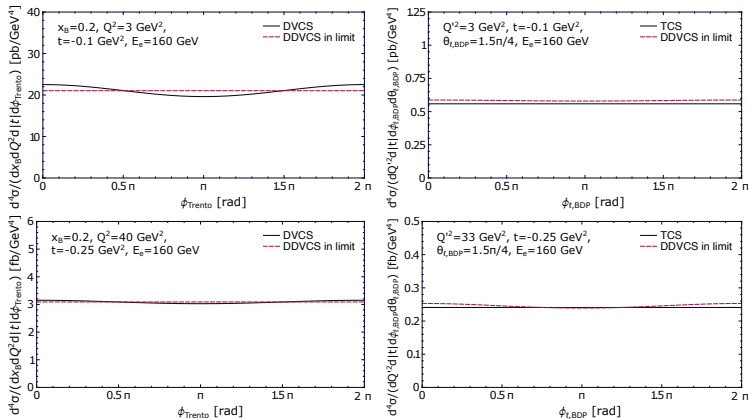
- Axial contribution:

$$i\mathcal{M}_{\text{DDVCS}}^{(A)} = \frac{-i}{2} \epsilon_{\perp}^{\mu\nu} j_{\mu}(s_\ell, \ell_-, \ell_+) j_{\nu}(s, k', k) \left[\tilde{\mathcal{H}} \mathcal{J}_{s_2 s_1}^{(1,5)+} + \tilde{\mathcal{E}} \frac{\Delta^+}{2M} \mathcal{J}_{s_2 s_1}^{(2,5)+} \right]$$

More details in:

K. Deja, V. Martínez-Fernández, B. Pire, P. Sznajder, J. Wagner, PRD **107** (2023), no. 9, 094035

DVCS & TCS limits of DDVCS



Comparison of DDVCS and (left) DVCS and (right) TCS cross-sections for pure VCS subprocess. **GK model for GPDs.**

Trento: PRD 70, 117504 (2004); **BDP:** EPJC23, 675 (2002)



Observables in DDVCS: beam-spin asymmetry

- Single beam-spin asymmetry for longitudinally polarized electrons:

$$A_{LU}(\phi_{\ell, \text{BDP}}) = \frac{\Delta\sigma_{LU}(\phi_{\ell, \text{BDP}})}{\sigma_{UU}(\phi_{\ell, \text{BDP}})}$$
$$\Delta\sigma_{LU}(\phi_{\ell, \text{BDP}}) = \int_0^{2\pi} d\phi \int_{\pi/4}^{3\pi/4} d\theta_{\ell, \text{BDP}} \sin\theta_{\ell, \text{BDP}}$$
$$\times \left(\frac{d^7\sigma^{\rightarrow}}{dx_B dQ^2 dQ'^2 d|t| d\phi d\Omega_{\ell, \text{BDP}}} - \frac{d^7\sigma^{\leftarrow}}{dx_B dQ^2 dQ'^2 d|t| d\phi d\Omega_{\ell, \text{BDP}}} \right)$$

- We consider $Q'^2 > Q^2$: our DDVCS is “more” timelike than spacelike
- Variable for later use:

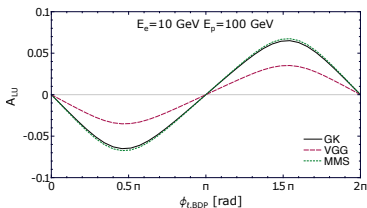
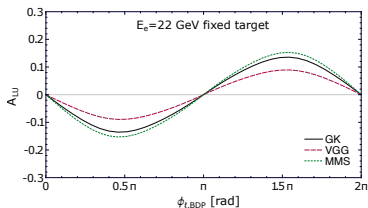
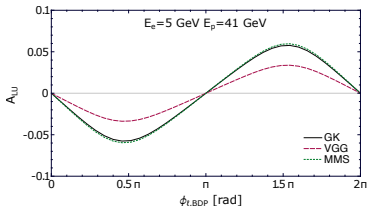
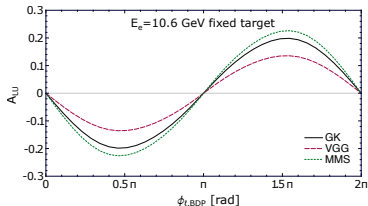
$$y = \frac{pq}{pk} \underbrace{=} \frac{E-E'}{E},$$

proton
rest
frame

E =energy of incoming electron beam, E' =energy of recoiled electron

Observables in DDVCS: beam-spin asymmetry

K. Deja, V. Martínez-Fernández, B. Pire, P. Sznajder, J. Wagner,
PRD 107 (2023), no. 9, 094035



JLab12, JLab20+: **15-20%**

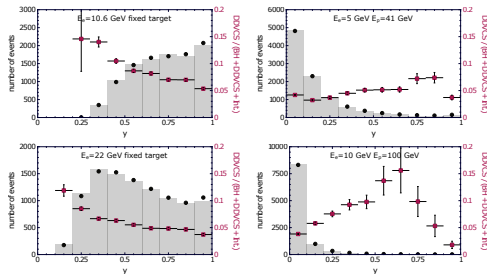
EIC 5x41, EIC 10x100: **3-7%**

Experiment	Beam energies [GeV]	y	$ t $ [GeV ²]	Q^2 [GeV ²]	Q'^2 [GeV ²]
JLab12	$E_e = 10.6, E_p = M$	0.5	0.2	0.6	2.5
JLab20+	$E_e = 22, E_p = M$	0.3	0.2	0.6	2.5
EIC	$E_e = 5, E_p = 41$	0.15	0.1	0.6	2.5
EIC	$E_e = 10, E_p = 100$	0.15	0.1	0.6	2.5



Monte Carlo study: distribution in y (DDVCS)

K. Deja, V. Martínez-Fernández, B. Pire, P. Sznajder, J. Wagner,
PRD **107** (2023), no. 9, 094035



JLab12, JLab20+

EIC 5x41, EIC 10x100

10000 events/distribution. Neither acceptance nor detectors response are taken into account in this study

■ EpIC MC
● integrated cross-section
■ pure DDVCS fraction

Kinematic cuts:

$$Q^2 \in (0.15, 5) \text{ GeV}^2$$

$$Q'^2 \in (2.25, 9) \text{ GeV}^2$$

$$\text{JLab: } -t \in (0.1, 0.8) \text{ GeV}^2$$

$$\text{EIC: } -t \in (0.01, 1) \text{ GeV}^2$$

$$\phi, \phi_\ell \in (0.1, 2\pi - 0.1) \text{ rad}$$

$$\theta_\ell \in (\pi/4, 3\pi/4) \text{ rad}$$

$$\text{JLab: } y \in (0.1, 1)$$

$$\text{EIC: } y \in (0.05, 1)$$



Experiment	Beam energies [GeV]	Range of $ t $ [GeV ²]	$\sigma_{ 0 < y < 1}$ [pb]	$\mathcal{L}^{10k} _{0 < y < 1}$ [fb ⁻¹]	y_{\min}	$\sigma_{ y_{\min} < y < 1} / \sigma_{ 0 < y < 1}$
JLab12	$E_e = 10.6, E_p = M$	(0.1, 0.8)	0.14	70	0.1	1
JLab20+	$E_e = 22, E_p = M$	(0.1, 0.8)	0.46	22	0.1	1
EIC	$E_e = 5, E_p = 41$	(0.05, 1)	3.9	2.6	0.05	0.73
EIC	$E_e = 10, E_p = 100$	(0.05, 1)	4.7	2.1	0.05	0.32

Worldwide picture

experiments

closed active planned

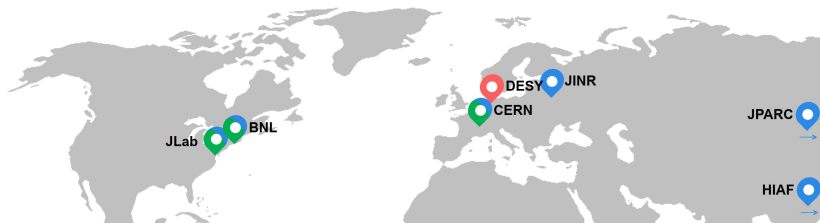
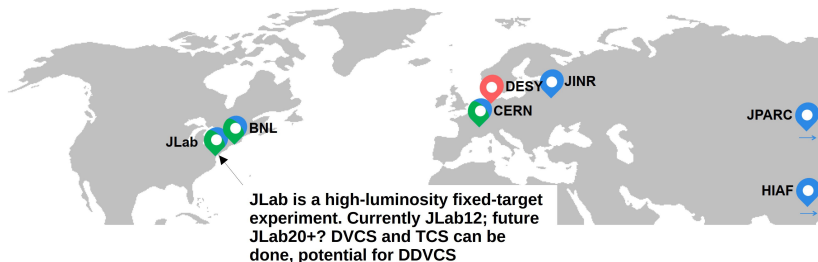


Image courtesy of Paweł Sznajder

Worldwide picture

experiments

closed active planned

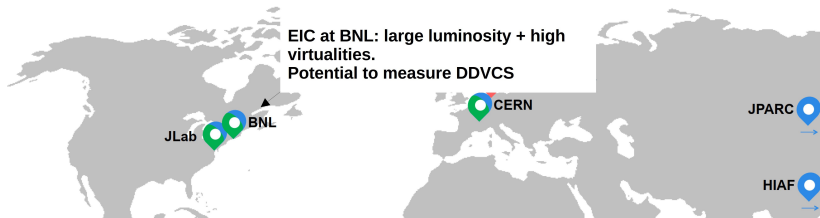


More info about JLab20+: A. Accardi et al., arXiv: nucl-ex/2306.09360

Worldwide picture

experiments

closed active planned



More info about EIC: R. Abdul Khalek et al., Nucl. Phys. A 1026 (2022) 122447 (Yellow Report)

Summary

- DIS and PDF have been explained and related
- GPDs as a 3D version of the PDFs have been introduced via exclusive inelastic scattering
- I have shown how DDVCS allows to map GPDs on their whole domain, i.e., $x \neq \xi$. Full knowledge of GPDs is fundamental in order to:
 - ① Understand the different sources for the spin of the hadron
 - ② Perform transverse imaging (tomography)
- The latest results in both the theoretical and phenomenological aspects of DDVCS have been discussed
- New experiments are ahead: EIC (and maybe JLab20+?)

Thank you!

Complementary slides

Light-cone coordinates

- A way to parameterize 4-vectors:

$$z^\mu = z^- n^\mu + z^+ n'^\mu + z_\perp^\mu,$$

$$n^2 = n'^2 = 0, \quad nn' \neq 0,$$

$$z_\perp n = z_\perp n' = 0$$

- n, n' define the “minus” and “plus” longitudinal directions, respectively

Wilson line

- It restores the gauge invariance of the PDF,

$$\mathcal{W}[z_1^-, z_2^-] = \mathbb{P} \exp \left[ig \int_{z_2^-}^{z_1^-} da^- A^+(a^-) \right]$$

- It is the result of resumming contributions to leading twist ($\mathcal{O}(\text{constant}/Q^2)$ neglected) from gluon exchanges between the hard part (parton-photon interaction) and the soft part (non-active partons):

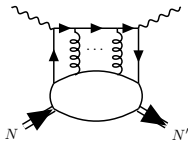


Diagram for a Wilson line

- Under the gauge $A^+ = 0$, $\mathcal{W} \equiv 1$ and can be disregarded

DVCS amplitude

- Photon-proton interaction, to order[†] $\mathcal{O}(\alpha_{\text{em}})$:

$$\begin{aligned} \langle \gamma(q') N(p') | S^{(2)} | \gamma^*(q) N(p) \rangle &= \frac{3}{4} (2\pi)^4 \delta(p+q-p'-q') (\varepsilon_{q\lambda})_\alpha (\varepsilon_{q'\lambda'}^*)_\beta \\ &\times \sum_f e_f^2 \int d^4\ell \frac{d^4z}{(2\pi)^4} e^{i\ell z} \text{tr} \left\{ \left[\gamma^\beta \frac{i(\ell+q)}{(\ell+q)^2+i0} \gamma^\alpha + \gamma^\alpha \frac{i(\ell-q')}{(\ell-q')^2+i0} \gamma^\beta \right] \gamma^\mu \right\} \\ &\times \langle N(p') | : \bar{q}_f(0) \gamma_\mu q_f(z) : | N(p) \rangle \\ &+ (\text{axial term}) \end{aligned}$$

- ℓ is the 4-momentum of the active parton
- $\varepsilon_{q\lambda}$ is the polarization vector of the photon with momentum q and polarization λ

[†] $e_f^2 = e^2 Q_f^2$, $Q_f =$ quark's fraction of proton electric charge

DVCS amplitude

- Momentum can be parameterized with the following variables:

① x , the fraction of the hadron longitudinal momentum that is carried away by the parton

② $\xi = -\frac{\Delta_{\bar{q}}}{2\bar{p}\bar{q}}$, called skewness

$$(\bar{p} = (p + p')/2, \Delta = p' - p, \bar{q} = (q + q')/2)$$

- This way, for instance,

$$(\ell - q')^\mu = (x - \xi)\bar{p}^+ n'^\mu + \left(\ell^- - \frac{Q^2}{4\xi\bar{p}^+}\right)n^\mu + \ell_\perp + \Delta_\perp$$

$$(\ell - q')^2 = -(x - \xi)\frac{Q^2}{2\xi} + \underbrace{\mathcal{O}\left(\frac{\ell_\perp^2}{Q^2}, \frac{\Delta_\perp^2}{Q^2}, \frac{\ell_\perp \Delta_\perp}{Q^2}, \frac{\ell^- \bar{p}^+}{Q^2}\right)}$$

Neglecting transverse dynamics renders collinear factorization

- Collinear factorization is justified on Q^2 being the scale of the process and, therefore, larger than any other momentum

GPDs of a spin-1/2 hadron

- Further decomposition of the correlator that has been called the GPD so far ($t = \Delta^2$):

$$F_f = \frac{1}{2} \int \frac{dz^-}{2\pi} e^{ix\bar{p}^+ z^-} \langle N(p') | \bar{q}_f(-z/2) \gamma^+ q_f(z/2) | N(p) \rangle \Big|_{\substack{z^+=0 \\ z_\perp=0}}$$
$$= \frac{1}{2\bar{p}^+} \left[H_f(x, \xi, t) \bar{u}(p') \gamma^+ u(p) + E_f(x, \xi, t) \bar{u}(p') \frac{i\sigma^{+\alpha} \Delta_\alpha}{2M} u(p) \right],$$
$$\sigma^{\beta\alpha} = \frac{i}{2} [\gamma^\beta, \gamma^\alpha]$$

- Technically, the GPDs are H_f and E_f , although F_f is usually referred to as the GPD too. As usual, it is a matter of context...
- The axial term give rise similarly to another two GPDs: \tilde{H}_f and \tilde{E}_f

Kleiss-Stirling (KS) techniques

- Define a massless spinor basis $\{u(\kappa_0, \pm)\}$ for momentum $\kappa_0^2 = 0$ and helicity \pm . The negative-helicity state is defined by:

$$\bar{u}(\kappa_0, -)u(\kappa_0, -) = \omega_{-\kappa_0}, \quad \omega_\lambda = \frac{1}{2}(1 + \lambda\gamma^5)$$

- Define a spacelike vector $\kappa_1^2 = -1$ such that $\kappa_0\kappa_1 = 0$, then the positive-helicity state is:

$$u(\kappa_0, +) = \kappa_1 u(\kappa_0, -)$$

Kleiss & Stirling, Nucl. Phys. B 262 (1985) 235-262

Kleiss-Stirling (KS) techniques

- For any spinor associated to a massless fermion of momentum p , imposing Dirac equation, projection

$$u(p, \lambda)\bar{u}(p, \lambda) = \omega_\lambda \not{p}, \quad \lambda = \pm,$$

and using spinor basis above, one finds:

$$u(p, \lambda) = \frac{\not{p}u(\kappa_0, -\lambda)}{\sqrt{2p\kappa_0}}$$

- The only restriction to this formula is $p\kappa_0 \neq 0$ and, for computer purposes, not extremely small
- Massive spinors can be expanded by means of the massless ones described here

Kleiss & Stirling, Nucl. Phys. B 262 (1985) 235-262

- **f = contraction of 2 currents**

$$f(\lambda, k_0, k_1; \lambda', k_2, k_3) = \bar{u}(k_0, \lambda) \gamma^\mu u(k_1, \lambda) \bar{u}(k_2, \lambda') \gamma_\mu u(k_3, \lambda') = 2[s(k_2, k_1)t(k_0, k_3)\delta_{\lambda-}\delta_{\lambda'+} + t(k_2, k_1)s(k_0, k_3)\delta_{\lambda+}\delta_{\lambda'-} + s(k_2, k_0)t(k_1, k_3)\delta_{\lambda+}\delta_{\lambda'+} + t(k_2, k_0)s(k_1, k_3)\delta_{\lambda-}\delta_{\lambda'-}]$$

- **g = contraction of a current with a lightlike vector a**

$$g(s, \ell, a, k) = \bar{u}(\ell, s) \not{a} u(k, s) = \delta_{s+} s(\ell, a) t(a, k) + \delta_{s-} t(\ell, a) s(a, k)$$

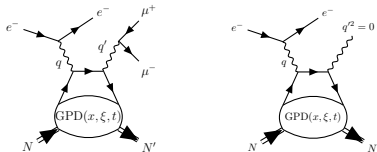
- **BH diagrams can be treated in a similar manner**

More details in:

K. Deja, V. Martínez-Fernández, B. Pire, P. Sznajder, J. Wagner, PRD **107** (2023), no. 9, 094035

DVCS limit of DDVCS

- DDVCS to DVCS:



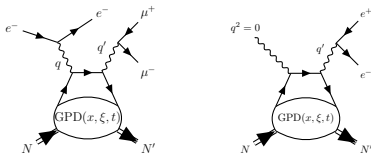
DDVCS (left), DVCS (right)

$$\int d\Omega_\ell \underbrace{\frac{d^7\sigma}{dx_B dQ^2 dQ'^2 d|t| d\phi d\Omega_\ell}}_{\text{DDVCS}} \xrightarrow{Q'^2 \rightarrow 0} \left(\underbrace{\frac{d^4\sigma}{dx_B dQ^2 d|t| d\phi}}_{\text{DVCS}} \right) \frac{\mathcal{N}}{Q'^2}$$

$$\mathcal{N} = \alpha_{\text{em}} / (3\pi)$$

TCS limit of DDVCS

- DDVCS to TCS:

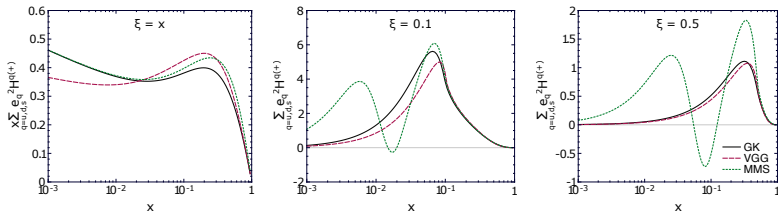


DDVCS (left), TCS (right)

$$\int d\phi \underbrace{\frac{d^7\sigma}{dx_B dQ^2 dQ'^2 d|t| d\phi d\Omega_\ell}}_{\text{DDVCS}} \xrightarrow{Q^2 \rightarrow 0} \underbrace{\left(\frac{d^4\sigma}{dQ'^2 d|t| d\Omega_\ell} \right)}_{\text{TCS}} \underbrace{\frac{d^2\Gamma}{dx_B dQ^2}}_{\text{EPA photon flux}}$$

$$\frac{d^2\Gamma}{dx_B dQ^2} = \frac{\alpha_{\text{em}}}{2\pi Q^2} \left(1 + \frac{(1-y)^2}{y} - \frac{2(1-y)Q_{\text{min}}^2}{yQ^2} \right) \frac{\nu}{E_{x_B}} \leftarrow \text{EPA photon-flux}$$

Models for the C-even part of GPD H^q



Distributions of $\sum_q e^{2iq} H^{q(+)}(x, \xi, t)$ at $t = -0.1 \text{ GeV}^2$, where $q = u, d, s$ flavors for (left) $\xi = x$, (middle) $\xi = 0.1$ and (right) $\xi = 0.5$. The solid black, dashed red and dotted green curves describe the GK, VGG and MMS GPD models, respectively. The C-even part of a given vector GPD is defined as:

$H^{q(+)}(x, \xi, t) = H^q(x, \xi, t) - H^q(-x, \xi, t)$. The scale is chosen as $\mu_F^2 = 4 \text{ GeV}^2$.